Biomechanical Study of Porous Osteotomy Block in Evans Osteotomy for Flat Foot Correction Based on Finite Element Method

Yang Baiyin[1a*], Xie Haiqiong[1b] and Gan Daoqi[1c]

[1]Chongqing University of Posts and Telecommunications, Chongqing, China

Abstract: ased on the finite element method, the effect of porous osteotomy block on the biomechanics of surrounding joints in the treatment of flat foot by Evans osteotomy is studied. The finite element method is used to simulate the osteotomy block for Evans osteotomy to correct flatfoot. The effect of Evans osteotomy on the foot force line is analyzed from the biomechanical point of view. The osteotomy blocks were divided into solid osteotomy blocks and porous osteotomy blocks, and normal foot and flat foot were used as control groups. The results show that Evans osteotomy can effectively improve the force line of the foot to correct the flat foot. Compared with the solid osteotomy block, the porous osteotomy block can also play a corrective effect and reduce the stress shielding effect when used for Evans osteotomy to correct the flat foot.

1 INTRODUCTION

Flatfoot is a postural deformity disease of the foot, which is characterized by medial longitudinal arch collapse and ankle complex deformity. The prevalence of flatfoot in adults may be as high as 23%[1]. Obesity, foot injury and fatigue can lead to the formation of flatfoot, and posterior tibial tendon dysfunction (PTTD) is considered to be the main cause of adult acquired flatfoot[2]. Due to the change of arch structure and the abnormality of biomechanical function in patients with flatfoot, it is easy to cause complications such as valgus, knee joint pain and Achilles tendinitis[3]. At present, the treatment methods for flatfoot are generally divided into non-surgical treatment and surgical treatment. Patients with mild conditions are often treated with non-surgical methods such as corrective insoles[4], which are more easily accepted by patients. For patients with severe disease or inactive foot joint stiffness, Evans osteotomy, Cotton osteotomy and arthrodesis are often used[5].

Evans osteotomy, also known as lateral column lengthening osteotomy, has a good therapeutic effect in correcting flat foot[6]. With the rapid development of science and technology and medical additive manufacturing (3D printing), as one of the important components of Evans osteotomy, the osteotomy block is gradually replaced by the porous osteotomy block of bionic human bone. Many studies have shown that biomechanical effects play an important role in the treatment and correction of foot diseases. With the development of computer technology, the research commonly used in foot biomechanics is generally cadaver experiment and finite element analysis. Although the former makes the experimental model reliable and accurate, the cost of the experiment is high, the efficiency is low and the ethics is violated. Therefore, finite element analysis is more and more widely used in the study of ankle biomechanics. Yinghu et al.used the finite element method to study the effects of five midfoot/hindfoot arthrodesis on foot biomechanics in walking posture[7]. Portilla et al.used an innovative finite element model to analyze the treatment of flatfoot with posterior foot joint replacement and three joint fusion[8]. Larrainzar-Garijo et al.[9] used the finite element model reconstructed from CT images of healthy patients to simulate the single foot support stage of adult walking, and evaluated the effect on the soft tissue of the arch according to clinical and biomechanical effects. Although the above work has studied the effects of surgical methods such as simulated arthrodesis on foot biomechanics, there is no biomechanical simulation study on osteotomy and analysis of the effects of implants on foot in surgical methods.

Therefore, the finite element model of Evans osteotomy is established in this study, and the solid osteotomy block is used as the control group to compare the simulation analysis with the porous osteotomy block. To study the effect of porous osteotomy on the surrounding joints in Evans osteotomy, to explore the advantages of porous osteotomy relative to solid osteotomy and the change of biomechanical position distribution by Evans osteotomy, and to provide preoperative guidance and visualization platform for doctors to choose this treatment method.

[a] S202131027@stu.cqupt.edu.cn
[b] xiehq@cqupt.edu.cn
[c] S202101024@stu.cqupt.edu.cn

2 MATERIALS AND METHODS

CT images of the right foot of a 28-year-old male patient with flat foot who weighed 70 kg and had no history of trauma and surgery were collected. The layer thickness and layer spacing were 0.5 mm and 1 mm, respectively, and the resolution is 512×512 pixels. A total of 355 images were output and stored in DICOM format. Informed consent was signed before the medical impact of the scan.

2.1 Establishment of finite element model

The establishment of finite element model of normal foot and flat foot is the same as that of Evans osteotomy finite element model. This paper only describes the establishment of finite element model of Evans osteotomy. The collected CT images were imported into Mimics Research20.0 for processing, and threshold segmentation, bone reconstruction, iterative smoothing and mirror extraction were performed to obtain a preliminary foot bone model, which was saved in STL format. Firstly, the geometric model of foot bone is established by optimizing the model with 3-matic software, removing the bad edges, holes and deformities of the model (see Figure 1). Secondly, the middle and posterior foot bone model and the designed osteotomy block model are imported into UG12.0 for assembly according to Evans osteotomy, and the cartilage surface is established on one side of the articular surface by using the stretching command, and Boolean operation is performed with the articular surface on the other side to create the articular cartilage model (see Figure 2), which is output in Step format. Finally, all the assembled geometric models are imported into HyperMesh2019 for finite element pre-processing operations such as meshing, and the finite element model of Evans osteotomy is obtained.

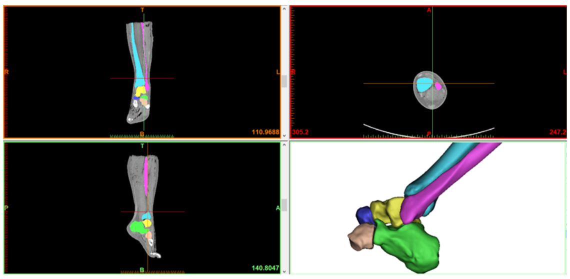

Figure 1: Image processed by Mimics 3D reconstruction.

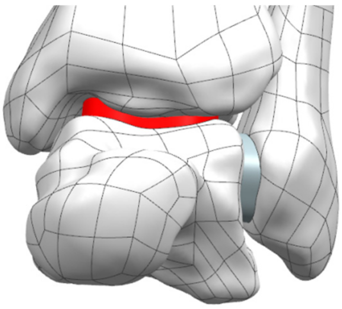

Figure 2: Schematic diagram of partial cartilage model.

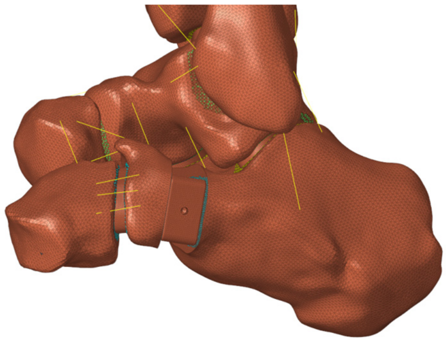

Figure 3: Foot finite element mesh model.

The final complete finite element model includes 6 bones (tibia, fibula, talus, calcaneus, cuboid, scaphoid) and 6 cartilages (tibiotalar articular cartilage, talofibular articular cartilage, posterior talocalcaneal articular cartilage, anterior and middle talocalcaneal articular cartilage, calcaneocuboid articular cartilage, talonavicular articular cartilage), middle and posterior foot ligament and osteotomy block. The mesh size of bone model is 1mm, the mesh size of cartilage model is 0.5mm, the mesh size of osteotomy block model is 0.5mm, and the yellow line is the T3D2 truss unit of simulated ligament. There are 149850 nodes, 683496 solid tetrahedral mesh elements and 33 truss elements (see Figure 3).

2.2 Material properties of the model

In the foot model, the articular cartilage and the middle and hind foot bones are set as isotropic linear elastic materials, and the relevant material parameters are taken from the literature[7,10]. The ligament is considered as an incompressible material that is only pulled. The solid osteotomy block is assigned titanium alloy material properties, which is also set to isotropic linear elastic material. The material properties of the porous osteotomy block were measured by uniaxial static compression test of 3D printed porous samples.

The preparation of porous samples is to use MSLattice to generate porous structures with different structures, different volume fractions and different unit sizes. The STL file of the generated porous structure is imported into Magics, and the cylindrical porous sample is generated by Boolean operation command. Finally, the designed porous sample is printed by electron beam melting (EBM) technology.

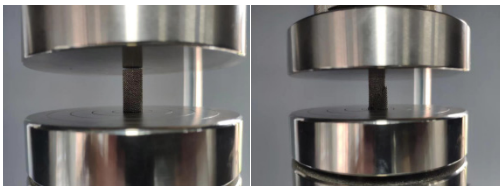

Figure 4: Uniaxial static compression experiment of porous sample.

Table 1: Material parameters.

	Elastic modulus(MPa)	Poisson ratio	Cross-sectional area(mm^2)
Bone	7300	0.3	—
Cartilage	1	0.4	—
Ligaments	260	—	18.4

 https://doi.org/10.1051/bioconf/20235901013

Entity	110000	0.34	—
Porous	681.47	0.34	—

Through the WANCE microcomputer control electronic universal testing machine, the porous sample is tested as shown in Figure 4. The average compression rate of the test is 1mm/min, and the test is completed when the strain of the porous sample reaches 60 % or completely destroyed. According to the uniaxial static compression test, the material properties of the porous structure with the best mechanical properties were selected to simulate the porous osteotomy block. Finally, all the material parameters required for each part of the finite element model are shown in Table 1.

2.3 Loads and boundary conditions

When the patient is standing in a normal neutral position, his foot share his own weight. The patient's weight is 70 kg, so his left foot needs to bear about 350 N vertical gravity. In order to simulate the static standing in neutral position, a vertical downward loading force of 350 N is applied on the cross section of tibia and fibula. The ratio of the force applied by tibia and fibula is 5 : 1, and a completely fixed constraint is applied at the bottom of the calcaneus. The scaphoid and the cuboid constrain their degrees of freedom on the y and z axes, so that they can only move freely on the x axis.

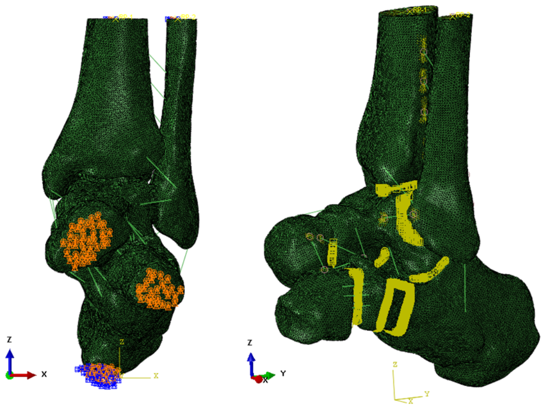

Figure 5: Foot finite element model; The picture on the left is a schematic diagram of loading and constraint, and the picture on the right is a schematic diagram of contact and binding.

The contact relationship between bone and articular cartilage is that one side of articular cartilage and bone is set as binding constraint, and the other side is set as friction contact. The friction coefficient between bone and articular cartilage is 0.01[11]. The contact relationship between the surface of the osteotomy block and the osteotomy plane on both sides is set as binding to avoid the osteotomy block slipping out. The two ends of the truss unit of the foot ligament, that is, the starting and ending points of the ligament, are coupled with the surrounding grid plane to simulate the starting and ending points of the ligament and reduce the stress concentration (see Figure 5).

3 RESULTS AND DISCUSSION

The set finite element model is imported into ABAQUS for analysis, and the ABAQUS implicit solver is used to solve the problem. The initial step size and the maximum incremental step of the analysis step are set to 0.01 and the large deformation switch is opened. It should be noted that the contact relationship between the articular cartilage and the bones on both sides adopts one end binding and one end friction. Therefore, a tolerance of 0.05 mm is set between the two friction surfaces when the contact surface is set, so as to avoid the risk that the simulation analysis cannot converge due to mutual penetration before the contact surface analysis.

Different material properties were given to the osteotomy block to simulate the solid osteotomy block and the porous osteotomy block for the finite element simulation of Evans osteotomy simulation. The stress distribution maps of some bones and osteotomy blocks when standing in neutral position were obtained and divided into solid group and porous group.

Table 2: Comparison of the maximum stress values of some bones in finite element model(MPa).

	talus	calcaneus	Osteotomy block
Normal foot	4.73	4.97	—
Flat foot	6.75	7.10	—
Entity group	4.85	5.11	6.38
Porous group	4.84	5.08	4.25

In the process of rear foot force in the neutral phase of gait, the force of tibia and fibula is transmitted downward through the tibiotalar joint, and then the ankle joint is transmitted through the talonavicular joint, calcaneocuboid joint and other front foot bones. Only the middle and rear foot are analyzed here. Therefore, the boundary conditions set in the simulation analysis are that the force of tibia and fibula is downward, the bottom of calcaneus is completely fixed, and the cuboid bone and scaphoid bone are partially constrained. The relevant data are collected as shown in Table 2.

The results of talus stress are shown in Figure 6. The talus stress distribution in the flat foot model is mainly concentrated in the lateral area of the tibiotalar joint surface and the talus neck. The talus stress distribution in the normal foot model and the Evans osteotomy model is mainly concentrated in the tibial joint surface and the talus neck.

The results of calcaneus stress are shown in Figure 7.The stress distribution of calcaneus in the flat foot model is mainly concentrated in the lateral side of the talocalcaneal joint surface and the fixation area of the sustentaculum tali and the bottom of the calcaneus. In the normal foot model, the stress distribution of the calcaneus is mainly concentrated in the talocalcaneal joint surface and the anterior side of the calcaneal tuberosity, the sustentaculum tali and the fixed area at the bottom of the calcaneus. In the Evans osteotomy model, the main concentration area of calcaneal stress distribution is similar to that of normal foot, and the stress distribution also appears at the osteotomy site and tends to the dorsal area.

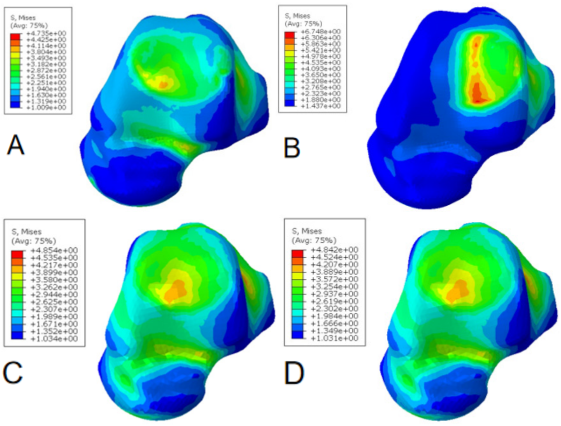

Figure 6: Stress distribution of talus; A is normal talus, B is flat talus, C is solid osteotomy block group, and D is porous osteotomy block group.

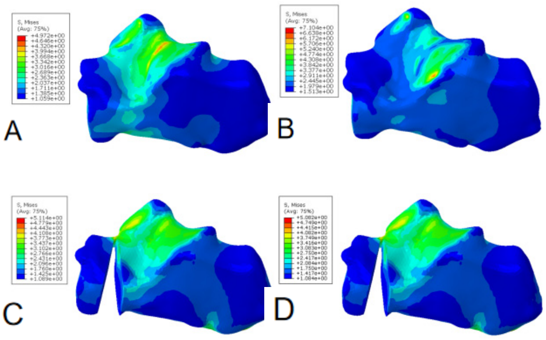

Figure 7: Stress distribution of calcaneus;A is normal calcaneus, B is flat calcaneus, C is solid osteotomy block group, and D is porous osteotomy block group.

The stress results of the osteotomy block are shown in Figure 8. The stress distribution of the porous osteotomy block is similar to that of the solid osteotomy block and is biased towards the dorsal region of the calcaneus.

Comparing the results of the four groups of simulation analysis, in the flat foot model, it can be seen that the bone stress of the middle and posterior foot has increased, which is significantly larger than that of the normal foot, and the stress distribution of the talus and calcaneus is biased to the outside, and the force line of the middle and posterior foot has shifted. Yinghu et al. used the finite element method to analyze five kinds of middle/posterior foot arthrodesis to correct flat foot. The study showed that the stress of each bone in the flat foot patients increased, and the peak pressure of the plantar increased significantly in each region, and the stress distribution is biased to the outside, which is consistent with the results of this study[7].

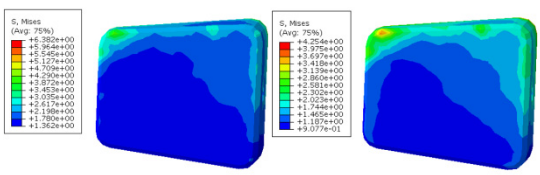

Figure 8: Stress distribution of osteotomy block; The left is a solid osteotomy, and the right is a porous osteotomy.

The bone stress distribution and stress size in the model of the simulated operation group were close to those of the normal foot. After the Evans osteotomy correction, the force line of the middle and posterior foot shifted from slightly to the outside to the normal force line of the middle and posterior foot. It can be seen that the Evans osteotomy is very obvious for the improvement of the force line of the posterior foot, and it is more inclined to correct the force line of the calcaneus valgus. In the model of simulated Evans osteotomy, the stress difference between the porous osteotomy block group and the talus and tibia is 0.59 MPa and 0.83 MPa, respectively, compared with the solid osteotomy block group. The stress difference between the solid osteotomy block and the talus and tibia is 1.53 MPa and 1.27 MPa, respectively. The stress difference between the porous osteotomy block and the adjacent bone is much smaller than that between the solid osteotomy block and the adjacent bone. It is verified that the porous osteotomy block is more conducive to reducing or optimizing the stress shielding effect under the same loading force and the same constraints.

The stress distribution of the osteotomy block shows that the force at the osteotomy site tends to be near the dorsal side when standing in a neutral position. Therefore, when considering Evans osteotomy, attention should be paid to preventing the implant of the osteotomy block from sliding from the dorsal side. Therefore, when performing Evans osteotomy, it is necessary to add a bone plate on the dorsal or lateral side or use a locking screw between the osteotomy block and the bilateral osteotomy to be fixed.

4 CONCLUSIONS

In this paper, the biomechanical response of Evans osteotomy for flat foot osteotomy is analyzed based on the finite element method combined with porous osteotomy block simulation, and the finite element simulation results of normal foot and flat foot are compared and analyzed. From the perspective of biomechanics, it provides reference guidance for preoperative clinicians to choose Evans osteotomy. The results show that Evans osteotomy can effectively improve the foot force line offset and foot bone stress caused by arch collapse caused by flat foot, and is more inclined to correct the force line of calcaneal valgus. The stress distribution of the osteotomy implant tends to the dorsal side. Under the same loading force and the same constraints, the porous osteotomy can also effectively improve the plantar force line and stress distribution and is more conducive to reducing or optimizing the stress shielding effect.

REFERENCES

1. Shibuya, N., Jupiter, D.C., Ciliberti, L.J. (2010) Characteristics of Adult Flatfoot in the United States. J.Journal of Foot & Ankle Surgery., 49: 363-368. https://doi.org/10.1053/j.jfas.2010.04.001.
2. Richie, D. (2020) Biomechanics and Orthotic Treatment of the Adult Acquired Flatfoot. J.Clinics in Podiatric Medicine and Surgery., 37: 71-89. https://doi.org/10.1016/j.cpm.2019.08.007.

3. Bertani, A., Cappello, A., Benedetti, M.G. (1999) Flat foot functional evaluation using pattern recognition of ground reaction data. J.Clinical Biomechanics., 14: 484-493. https://doi.org/10.1016/s0268-0033(98)90099-7.
4. Choi, J.Y., Hong, W.H., Suh, J.S. (2020) The long-term structural effect of orthoses for pediatric flexible flat foot: A systematic review. J.Foot and Ankle Surgery., 26: 181-188. https://doi.org/10.1016/j.fas.2019.01.007.
5. Caroline, J.L., Michael, S.H. (2016) Adult flat foot deformity. J.Orthopaedics and Trauma., 30: 41-50. https://doi.org/10.1016/j.mporth.2016.02.005.
6. Viegas, G.V. (2003) Reconstruction of the pediatric flexible planovalgus foot by using an Evans calcaneal osteotomy and augmentative medial split tibialis anterior tendon transfer. J.The Journal of Foot and Ankle Surgery., 42: 199-207. https://doi.org/10.1016/S1067-2516(03)70029-5.
7. Yinghu, P., Wenxin, N., Wai-Chi Wong, D. (2021) Biomechanical Comparison among Five Mid/hindfoot Arthrodeses Procedures in Treating Flatfoot Using a Musculoskeletal Multibody Driven Finite Element Model. J.Computer Methods and Programs in Biomedicine., 211: 106408. https://doi.org/10.1016/j.cmpb.2021.106408.
8. Portilla, C., Larrainzar-Garijo, R., Bayod, J. (2020) Analysis of biomechanical stresses caused by hindfoot joint arthrodesis in the treatment of adult acquired flatfoot deformity: A finite element study. J.Foot and Ankle Surgery., 26: 412-420. https://doi.org/10.1016/j.fas.2019.05.010.
9. Larrainzar-Garijo, R., Cifuentes de la Portilla, C., Gutiérrez-Narvarte, B. (2019) Effect of the calcaneal medializing osteotomy on soft tissues supporting the plantar arch: A computational study. J.Revista Española de Cirugía Ortopédica y Traumatología., 63: 155-163. https://doi.org/10.1016/j.recote.2019.02.001.
10. Siegler, S., Block, J., Schneck, C.D. (1998) The mechanical characteristics of the collateral ligaments of the human ankle joint. J.Foot & Ankle., 8: 234-242. https://doi.org/10.1177/107110078800800502.
11. Cheung, T.M., Zhang, M., Leung, K.L. (2005) Three-dimensional finite element analysis of the foot during standing—a material sensitivity study. J.Journal of Biomechanics., 38: 1045-1054. https://doi.org/10.1016/j.jbiomech.2004.05.035.